THE JOURNAL OF PHYSICAL CHEMISTRY B

Article

pubs.acs.org/JPCB

Structural Effects of the β-Vinyl Linker in Pyridinium Porphyrins: Spectroscopic Studies in Organic Solvents and AOT Reverse Micelles

Vanda Vaz Serra,*[,†,‡] Suzana M. Andrade,[†] Eduarda M. P. Silva,[‡] Artur M. S. Silva,[‡] Maria G. P. M. S. Neves,[‡] and Sílvia M. B. Costa*[,†]

[†]Centro de Química Estrutural, Complexo I, Instituto Superior Técnico, Universidade Técnica de Lisboa, Av. Rovisco Pais, 1049-001 Lisboa, Portugal

[‡]Departamento de Química & QOPNA, Universidade de Aveiro, Campus Universitário de Santiago, 3810-193 Aveiro, Portugal

Supporting Information

ABSTRACT: Two isomeric β-vinylpyridinium porphyrins, 2-[2-(2-methylpyridinium)-vinyl]-5,10,15,20-tetraphenylporphyrin (**1**, *ortho* isomer) and 2-[2-(4-methylpyridinium)-vinyl]-5,10,15,20-tetraphenylporphyrin (**2**, *para* isomer), which have shown different photodynamic behavior were investigated in organic solvents and sodium 1,4-bis(2-ethylhexyl)sulfosuccinate (AOT) reverse micelles. In organic systems, the absorption spectra present a red-shifted band that is more intense in the *para* isomer, in addition to the usual Soret band. This new band presents interesting solvatochromic effects which obey the multiparametric Kamlet−Taft equation. In AOT reverse micelles, the *ortho* isomer exhibits a strong dependence with the parameter $\omega_0 = [H_2O]/[AOT]$ which indicates that the molecule resides at the interface toward the organic phase. By contrast, no evidence was detected for the encapsulation of *para* isomer **2** in AOT reverse micelles. The hypothesis of two ground state isomers with different contributions of *trans* and *quinoid* structures is advanced on the basis of the overall data collected from electronic absorption, steady-state, and transient-state fluorescence emission. A charge transfer state in which an electron is fully transferred from the porphyrin to the pyridinium moiety is associated to a *quinoid* structure in isomer **2**. The *trans/quinoid* relative proportions may be accounted for by the orientation of the *ortho*-/*para*-pyridinium isomers relatively to the porphyrin core.

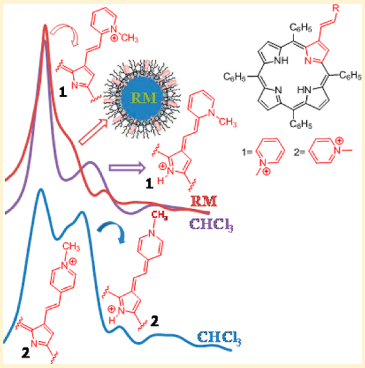

1. INTRODUCTION

In the last decades, interdisciplinary studies concerning porphyrin macrocycles pointed out their great potential applications in such fields as medicine, catalysis, and new electronic materials.[1] All those applications are strongly dependent on the macrocycle structure. Therefore, porphyrinoid research has been directed nowadays toward the development and photophysical/photochemical evaluation of novel functionalized porphyrins with improved molecular characteristics.

Photodynamic therapy (PDT) of oncological and non-oncological diseases is undoubtedly the most relevant area concerning applications. Some porphyrin derivatives are currently in use and others in advanced phases of clinical trials.[1] Considering the efficiency of PDT in the selective inactivation of microorganisms, some of us reported an easy synthetic route to cationic porphyrins **1** and **2** (Scheme 1) and their photodynamic activity against *Herpes simplex* virus type 1 (HSV-1).[2,3] Unexpectedly, while compound **1** is an efficient photosensitizer, compound **2** displays no virucidal effect under the same experimental conditions. The structural difference between these two free-base isomers is in the position of the porphyrin linkage to the pyridinium moiety. Compound **1** (*ortho* isomer) bears a 2-*N*-methylpyridinium linked covalently to a β-vinyl-*meso*-tetraphenylporphyrin, while compound **2** (*para* isomer) bears a 4-*N*-methylpyridinium moiety.

Scheme 1. Molecular Structures of Free Base β-Vinylpyridinium Porphyrins 1 and 2

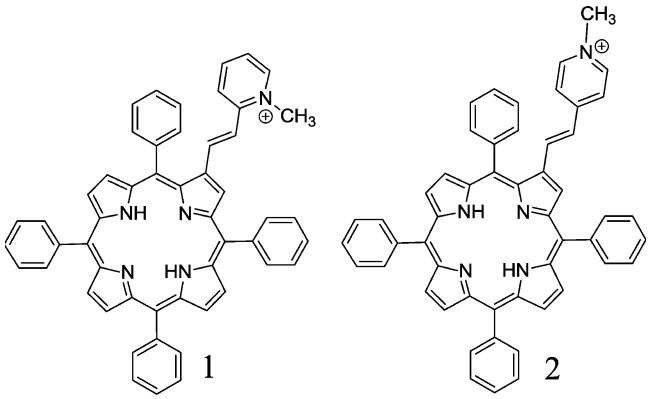

In the present study, we attempt to characterize the electronic properties of these two isomers. Knowing that

Received: August 1, 2013
Revised: October 29, 2013
Published: October 31, 2013

biological activity may involve mechanisms of membrane partitioning, we undertook a detailed photophysical study of **1** and **2** in neat organic solvents and also in AOT anionic reverse micelles often used as mimetic models to investigate different probes in membranes and interfaces. Important questions to be addressed are the identification of the structure of β-vinylporphyrins in different environments and to gather some insight on how different structures may influence their photodynamic activity.

2. EXPERIMENTAL SECTION

Sample Preparation. Stock solutions of compounds **1** and **2** (200 mM) in spectroscopic dimethyl sulfoxide DMSO (0.25 mM) were prepared, stored in the dark, and used within a month of preparation. The samples used in the solvatochromic assays were prepared by mixing small aliquots of stock solution of porphyrins **1** and **2** in DMSO in spectroscopic grade organic solvents, keeping the final DMSO concentration less than 1%. To avoid trace amounts of hydrochloric acid, organochloride spectroscopic solvents were passed through a column of neutral alumina prior to filtration over filter paper.

AOT, <99% purity, was purchased from Sigma-Aldrich and used as received. AOT reversed micelles were prepared using spectroscopic grade *iso*-octane and bidistilled water.

Spectroscopic Data. The electronic extinction spectra were recorded in a Jasco V-560 UV−vis absorption spectrophotometer. Resonance light scattering (RLS) spectra were carried out in a Perkin-Elmer LS50B spectrofluorimeter, by synchronous excitation and emission scanning in the right angle geometry, and corrected by subtracting the corresponding blank sample. Fluorescence steady-state measurements were performed in the same instrument. Corrected spectra were obtained using the correction file provided with the instrument. The spectra were recorded at room temperature using a 1 cm path length quartz cuvette.

The ^{1}H NMR spectra were recorded on a Bruker Avance 300 at 300.13 MHz, using $CDCl_3$ or $CDCl_3/CH_3OH$ (1:1) as solvent and TMS as internal reference.

Fluorescence Lifetime Measurements. Fluorescence lifetimes were obtained with a time-correlated single-photon counting (TC-SPC) technique using a commercial equipment FluoroLog-3 spectrofluorimeter (Horiba Jobin Yvon). Excitation at 445 nm was achieved using a NanoLED (fwhm <1.0 ns), at a repetition rate of 1 MHz. Individual photons were detected by a Hamamatsu R928 photomultiplier tube, and arrival times were stored in 4096 channels of an IBH Data Station Hub photon counting module. The data rate was set proportional to the source repetition rate up to ~2% to avoid photon pileup artifacts. Typical measurements involved accumulation of a maximum count per channel of at least 10 000. The instrument response function was obtained with a suspension of Ludox (colloidal silica beads) in water. Data analysis was performed by a deconvolution method using a non-linear least-squares fitting program, based on the Marquardt algorithm. Global analysis was made with the software package of Fluofit version 4.2 from PicoQuant. The goodness of the fit was evaluated by the usual statistical criteria and by visual inspection of the weighted residuals distribution and the autocorrelation function.

3. RESULTS

3.1. Absorption and Fluorescence Spectra in Organic Solvents. The electronic spectra of compounds **1** and **2** show striking differences likely related to their structural differences (Figure 1). In addition to the typical absorption bands of *meso*-

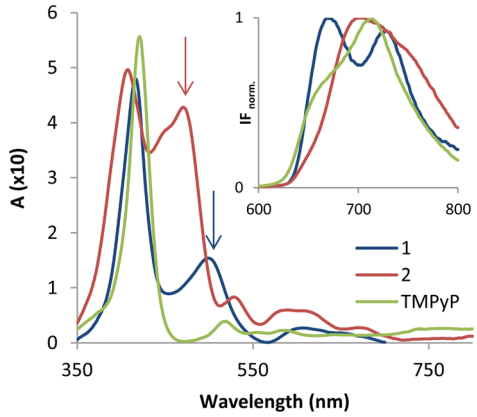

Figure 1. Absorption spectra of free base β-vinylpyridinium porphyrins **1** and **2** ($CHCl_3$; 5 μM) and TMPyP (water; 5 μM). Inset: normalized emission spectra at λ_{exc} = 400 nm. Arrows indicate the new red shift band.

tetrarylporphyrins, such as an intense Soret band around 400 nm and different components of the Q band at lower energies (500−700 nm), porphyrin **1** exhibits a new red shift band relative to the Soret. A similar but much more intense feature is observed in the absorption spectrum of compound **2**. Herein, a blue shift of all absorption bands associated with a pronounced increase in the intensity of the new band is detected. The emission profiles of compounds **1** and **2** in $CHCl_3$ are less complex than the absorption spectra, with structured Q(0,0) and Q(0,1) bands and wavelength maxima typical of *meso*-tetrarylporphyrins. The change of the *N*-methyl group position from *ortho* (compound **1**) to *para* (compound **2**) relatively to the porphyrin linking carbon shifts the emission wavelength maxima to lower energy, probably as a consequence of an increase in the β conjugation length.

For comparison, the absorption and emission spectra of the most studied *meso*-tetrarylpyridinium porphyrin, TMPyP, which has four *N*-methylpyridinium substituents in the *meso* positions, are also included in Figure 1. In this compound, the most significant difference is the absence of the new red shift band.

In order to study the influence of the surrounding media in the photophysical properties of β-vinylpyridinium porphyrins **1** and **2**, their absorption and emission spectra were measured in nine organic solvents (Figures S1, Supporting Information). After deconvolution of the Soret band into its Gaussian components (Figure S2, Supporting Information), the data collected from wavelength maxima are summarized in Table 1, taking into account the spectrophotometer error.

The solvatochromism of compounds **1** and **2** is readily apparent. Although the general profile of the absorption/emission spectra remains the same in different solvents, the wavelength maxima are very sensitive to changes in the solvent polarity, as expected for charge transfer states. As a general tendency, the increase in the solvent polarity results in blue shifts of both absorption and emission bands, but some exceptions can be found (Table 1). The absorption/emission wavelength maxima do not vary linearly with the solvent polarity, but a regular trend is observed in the difference of the wavelength maxima ($\Delta\lambda$) between the Soret and the new band

dx.doi.org/10.1021/jp4076993 | J. Phys. Chem. B 2013, 117, 15023−15032

Table 1. Absorption (λ_{abs}^{max}) and Emission Maxima (λ_{max}^{emi}) Obtained for Compounds 1 and 2 in Organic Solvents after Deconvolution of the Soret Region into Its Gaussian Components

	compound 1		compound 2	
solvent	λ_{abs}^{max} (±0.5 nm)	λ_{max}^{emi} [a] (±0.5 nm)	λ_{abs}^{max} (±0.5 nm)	λ_{max}^{emi} [b] (±0.5 nm)
chloroform	418.0; 504.0	661.0; 735.0	408.0; 475.0	694.0; 748.5
dichloromethane	416.0; 502.0	661.0; 735.0	411.5; 465.0	689.0; 741.5
octanol	415.5; 483.0	660.0; 730.0	421.0; 464.0	691.0; 744.5
hexanol	414.0; 480.0	660.0; 729.0	421.5; 467.0	691.0; 747.0
propanol	412.0; 475.0	663.0; 738.0	420.5; 462.0	690.0; 750.0
ethanol	410.0; 473.0	661.0; 729.0	420.0; 457.0	688.0; 747.0
methanol	410.0; 468.0	661.0; 730.0	420.0; 453.0	686.0; 744.0
acetonitrile	413.5; 468.0	655.0; 718.5	431.0; 457.0	682.0; 736.0
dimethyl sulfoxide	424.0; 457.0	658.5; 679.0	435.5; 460.0	682.0; 738.0

[a] λ_{exc} = 490 nm. [b] λ_{exc} = 470 nm.

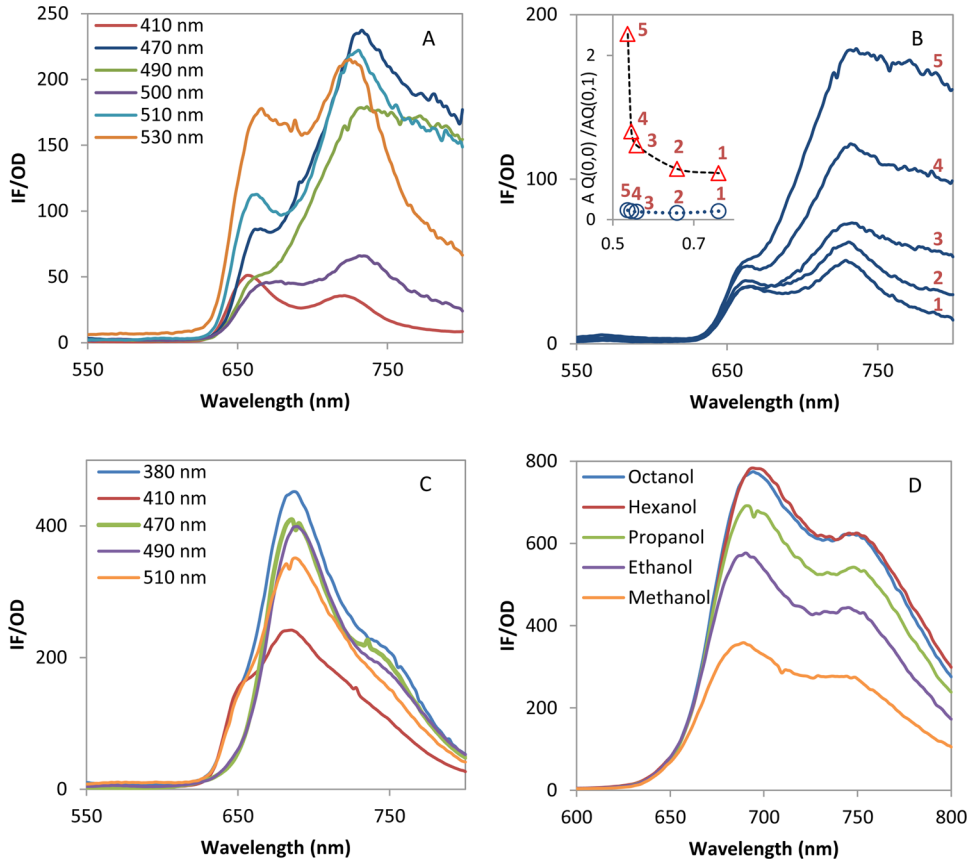

Figure 2. Fluorescence emission spectra of compounds **1** and **2**. (A, C) Dependence on the excitation wavelength in octanol for **1** (A) and **2** (C); (B, D) dependence on the alcohol chain length for **1** (B; λ_{exc} = 490 nm) and **2** (D, λ_{exc} = 470 nm). (1) methanol; (2) ethanol; (3) propanol; (4) hexanol; (5) octanol. The inset shows the variation of the ratio of Q(0,1) and Q(0,0) emission band area with solvent polarity for compound **1** (△) and compound **2** (○).

upon an increase in the solvent dielectric constant (see Figure S3, Supporting Information). It is also noteworthy that, among the solvents used, for compound **1**, the absorption spectral shifts are markedly more pronounced for the new band (46 nm) than for the characteristic Soret band (14 nm). This effect is reduced in compound **2**, as comparable spectral shifts are obtained for both bands (23 nm for the new band and 27 nm for the Soret band).

A detailed analysis of the emission profiles of compound **1** reveals that alcoholic solvents induce large and intriguing spectral changes that are dependent on the excitation wavelength (Figure 2A). It is worth mentioning an increase in the emission intensity of the Q(0,1) band at 730 nm relatively to the Q(0,0) band when exciting at λ_{exc} = 470 and 490 nm. Interestingly, this band increases linearly with the alcohol chain length (Figure 2B). Replacement of methanol by octanol gives the most intense Q(0,1) emission band which is about twice that of methanol. By contrast, the emission spectrum of compound **2** (Figure 2D) only displays a modest increase in the emission quantum yield.

The excitation spectra of compounds **1** and **2** in alcoholic solvents gave valuable information about the molecule's ground state. For compound **1**, the major point is the indication that the band in the range 468−483 nm (see Table 1) has no or

dx.doi.org/10.1021/jp4076993 | J. Phys. Chem. B 2013, 117, 15023−15032

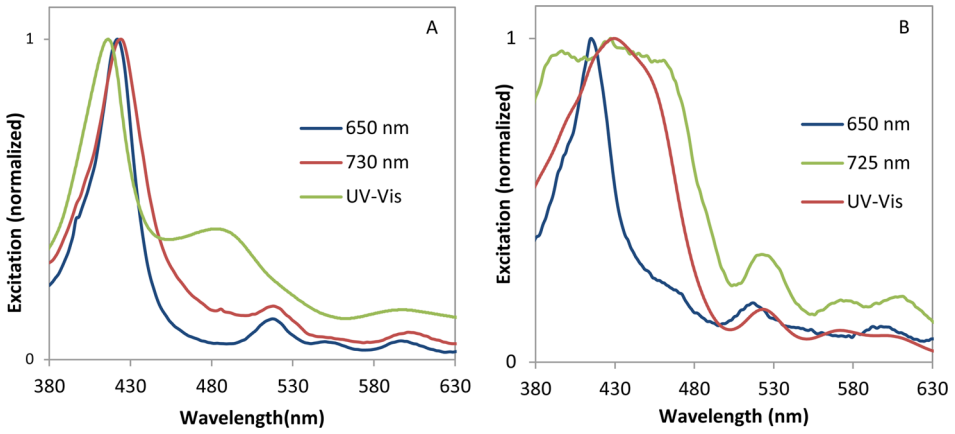

Figure 3. Excitation spectra of compound **1** in octanol collected at emission wavelengths of 650 and 730 nm (A) and **2** in methanol collected at emission wavelengths of 650 and 725 nm (B).

Table 2. Fluorescence Lifetimes of Compounds 1 and 2 in Neat Organic Solvents, λ_{exc} = 445 nm[a]

		compound **1**				compound **2**				
		A_1 (%)	A_2 (%)	A_3 (%)	χ^2	τ_1 (ns)	τ_2 (ns)	A_1 (%)	A_2 (%)	χ^2
acetonitrile	a	67.2	25.7	7.2	1.13	8.8	3.8	16.0	84.0	1.02
	c	nd	nd	nd	nd	8.3	3.6	5.2	94.8	0.95
dichloromethane	a	59.1	5.2	35.7	1.30	7.2	3.4	41.3	58.7	1.03
	c	nd	nd	nd	nd	7.3	1.8	2.9	97.1	0.95
chloroform	a	46.2	9.9	43.9	1.09	7.7	1.9	15.7	84.3	1.08
	c	nd	nd	nd	nd	6.7	3.0	21.4	78.6	0.95
DMSO	a	30.4	29.3	40.3	1.07	10.3	4.3	28.3	71.7	1.06
	c	nd	nd	nd	nd	9.2	3.8	12.9	87.1	0.93
methanol	a	53.4	18.5	28.1	1.10	9.3	4.2	44.4	55.6	1.05
	b, c	51.2	30.4	18.4	1.15	7.7	2.4	3.8	96.2	0.84
ethanol	a	60.9	27.6	11.5	1.04	9.3	4.2	44.4	55.6	1.05
	b, c	42.6	37.0	20.4	1.07	8.6	3.4	4.0	96.0	0.92
propanol	a	37.2	27.1	35.7	1.01	8.6	3.9	26.7	73.3	1.05
	b, c	24.5	31.9	43.6	1.08	8.7	3.9	5.9	94.1	0.90
hexanol	a	36.2	37.0	26.8	1.03	9.4	4.1	33.1	66.9	1.04
	b, c	23.4	29.9	46.7	1.18	9.1	4.0	10.8	89.2	0.96
octanol	a	36.2	38.6	25.2	1.13	10.1	4.6	37.9	62.1	1.02
	b, c	18.7	27.1	54.2	1.19	10.1	4.4	14.4	85.6	0.99

[a](a) λ_{em} = 650 nm; (b) **1**: λ_{em} = 730 nm. (c) **2**: λ_{em} = 680 nm; nd = not determined. τ_1 = 5.2 ns, τ_2 = 10.4 ns; τ_3 = 1.4 ns.

little contribution to the emission profiles, as can be seen by the absence of this band in the excitation spectra in octanol collecting the emission obtained at 650 and 730 nm, respectively (Figure 3A). On the other hand, the excitation spectra of compound **2** (Figure 3B), obtained from 650 and 725 nm, clearly show different profiles suggesting the existence of more than one species in the ground state (see discussion below). The excitation spectrum from 650 nm is dominated by a Soret band at 422 nm. The excitation spectrum from 725 nm is broader (Figure 3B), and is clearly the result of the overlap of the corresponding absorption spectra.

3.2. Fluorescence Lifetimes in Organic Solvents. Fluorescence lifetimes of compounds **1** and **2** measured in pure organic solvents are summarized in Table 2. Mono-exponential decays were never observed for both isomers. The fluorescence lifetimes found for compound **1** were independent of the emission wavelengths and on solvent nature, allowing a global fit analysis with fixed fluorescence lifetimes. A triexponential decay is always obtained with a short-lived component of 1.4 ns, an intermediate component lifetime of 5.2 ns, and a contribution of a longer lifetime of 10.4 ns.

For compound **2**, the decay was best fitted with a sum of two exponentials with one component of about 4 ns and another one of 9 ns. In this case, such global analyses do not give a good fitting for compound **2**. In contrast to compound **1**, now the ~4 ns lifetime component has a higher contribution (~90%), in polar protic and aprotic solvents. This component likely reflects a charge transfer state nature which may be assigned to the *para* isomer. Typical examples of fluorescence decays and respective fittings are shown in the Supporting Information (Figure S4).

3.3. Solvatochromism Studies. Solvatochromic scales have been widely used to understand and relate the solvent properties with the spectral shifts in the absorption and emission spectra of organic compounds. We have analyzed the spectral shifts of absorption and emission wavelength maxima of compounds **1** and **2** (Table S1, Supporting Information) in nine different solvents according to well-known solvatochromic models: Reichardt's parameter (E_T^N)[4,5] and the multiparametric model suggested by Taft et al. (KAT).[6]

The E_T^{30} scale, first proposed by Reichard and Dimroth, is based on the $\pi-\pi^*$ absorption band of a pyridinium-*N*-phenoxide betaine dye that responds to the change of the

dx.doi.org/10.1021/jp4076993 | J. Phys. Chem. B 2013, 117, 15023−15032

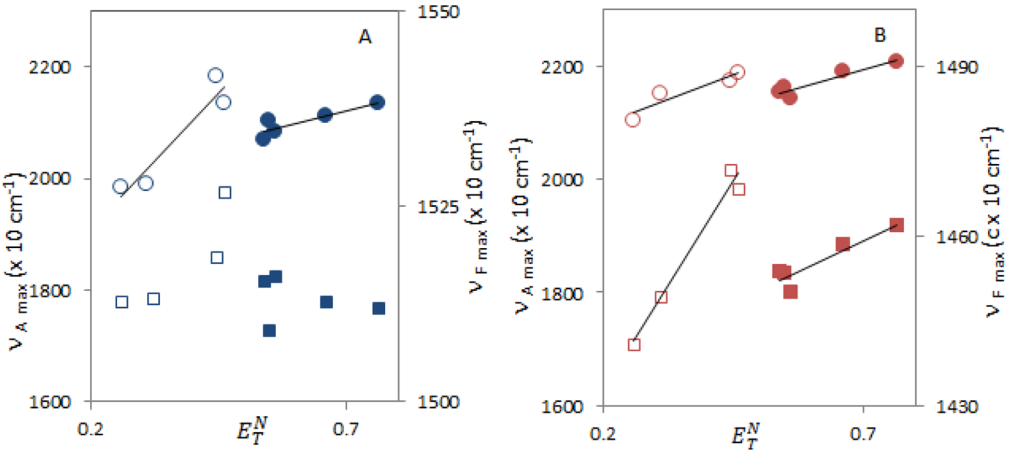

Figure 4. Maxima absorption (circles) and emission (squares) maxima in aprotic (open symbols) and protic solvents (closed symbols) of compound **1** (part A) and compound **2** (part B) vs E_T^N values.

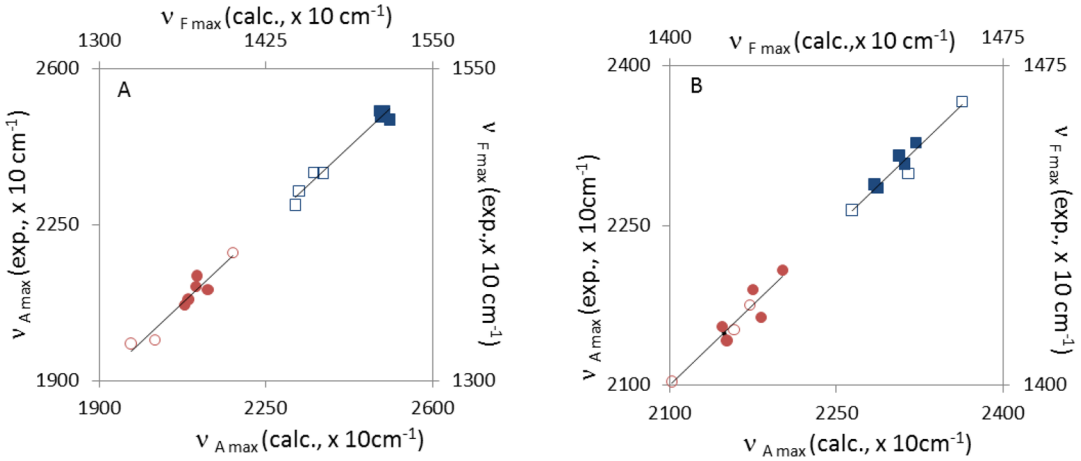

Figure 5. Experimental vs calculated absorption (circles) and emission (squares) wavenumber maxima of porphyrin **1** (A) and porphyrin **2** (B), using the KAT equation (eq 1) in aprotic (open symbols) and protic (closed symbols) solvents.

Table 3. Least Squares Correlations Fitted to the KAT Solvatochromic Equation for β-Vinylpyridinium Porphyrins 1 and 2

compound	absorption	emission
1	λ_{max} (nm) = $-17.4\alpha - 40.8\beta - 62.7\pi^* + 552.3$	λ_{max} (nm) = $-26.3\alpha - 20.7\beta - 3.4\pi^* + 700.3$
2	λ_{max} (nm) = $-25.7\alpha - 4.2\beta - 42.3\pi^* + 500.9$	λ_{max} (nm) = $-5.6\alpha - 4.8\beta - 23.1\pi^* + 708.9$

solvent polarity with a large shift. This scale (kcal/mol) depends on solvent dielectric properties and on the solvent hydrogen bonding capacity but is not affected by the solvent hydrogen bonding acceptor capacity. In our calculation, we have used a dimensionless normalized E_T^{30} value, the E_T^N parameter, that was only introduced afterward in order to avoid the use of a non-SI unit (kcal/mol).[7]

The variation of the absorption maxima of compounds **1** and **2** with E_T^N parameter (Figure 4) shows an almost linear trend with only a few deviations: acetonitrile, DMSO, and dichloromethane.

Unlike compound **2**, no linear correlation was found for the emission wavelength maxima of compound **1** with E_T^N. Instead, a sigmoidal curve with an inflection point that marks the frontier between the aprotic and protic media was obtained when plotting the areas of the emission bands (Q(0,1)/Q(0,0)). The experimental results indicate that the solvatochromism in the two β-vinylpyridinium porphyrins studied reflects different characteristics, in particular for compound **1**. In this compound, the positive charge on the nitrogen adjacent to the negative neighbor carbon may lead to specific interactions such as hydrogen bonding with alcohols.

In order to assess separately the effects of polarity and hydrogen bonding capacity to describe the complete picture of all intermolecular forces in the observed spectral shifts, we have used a multiparametric approach that comprises non-specific as well as specific solute−solvent interactions separately. The maximum absorption and emission wavelengths were then related with the Kamlet−Taft model as described in eq 1

$$\nu = \nu_0 + s(\pi^* + \delta) + a\alpha + b\beta \quad (1)$$

where ν and ν_0 are the calculated and experimental wavenumber maxima, s, a, and b are the coefficients determined from multiple linear regression analysis and are characteristic of the solute, α is the hydrogen-bond donation ability of the solvent, β is the hydrogen-bond acceptance ability of the solvent, π^* is a parameter that describes the polarity and polarizability of the solvent, and δ is a correction term

dx.doi.org/10.1021/jp4076993 | J. Phys. Chem. B 2013, 117, 15023−15032

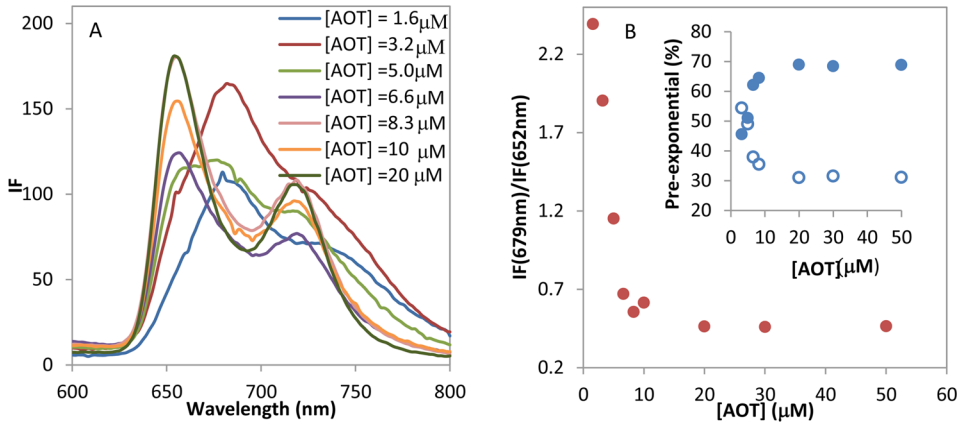

Figure 6. Variation of the emission spectra (A); (B) emission intensity and pre-exponential factors (inset, @ 5.0 ns (○) and @ 9.6 ns (●)) with AOT concentration for compound **1**.

introduced to account for different polarizabilities of solvent classes.

Good correlations (Figure 5) were found between the absorption and fluorescence wavenumbers calculated by the multicomponent linear regression by employing the KAT model and the experimental data (including DMSO, acetonitrile, and dichloromethane), and thus, this approach seems more adequate than the E_T^N scale to describe the solvatochromism of β-vinylpyridinium porphyrins. Important conclusions arise from the comparison of theoretical values obtained for compounds **1** and **2** (Table 3, in nanometers): (i) The major coefficient affecting the new absorption band of β-vinylpyridinium porphyrins is that describing the polarity/polarizability of the solvent π^*. (ii) Although π^* is also the major factor affecting the fluorescence spectrum of **2**, its contribution to the solvatochromism of the emission bands of compound **1** is very small. Further analysis of the correlation equation clearly suggests that hydrogen bond donation and acceptance parameters are the major factors which can explain the solvatochromic properties of the excited state of compound **1**. (iii) Negative solvatochromism is prompted by increasing values of α, β, and π^*.

3.4. AOT Reverse Micelles. The interesting differences observed in the photophysical properties of compounds **1** and **2** and its relation to the contributions of the solvent hydrogen bonding/accepting properties prompted us to study the photophysical properties of β-vinylpyridinium porphyrins **1** and **2** in reverse micelles. Since compounds **1** and **2** are cationic porphyrins, we chose anionic AOT reverse micelles which are generally characterized by the parameter $\omega_0 = [H_2O]/[AOT]$.[8−10] The absorption and the emission spectra of compound **2** are essentially unchanged in AOT reverse micelles and in AOT/*iso*-octane. Only a very small shift in the absorption and emission spectra could be detected, probably due to changes in the medium polarity. This behavior is indicative of a lack of partition between porphyrin **2** with the micelle interface and organic solvent.

The spectroscopy of porphyrin **1** was studied in a wide range of AOT concentrations. Then, absorption and emission techniques were used to evaluate the differences sensed by the molecules upon the formation of reverse micelles by addition of water.

3.4.1. Effect of AOT Concentration. At lower AOT concentrations in *iso*-octane (<1.6 μM), porphyrin **1** showed an absorption spectrum with a maximum detected at 490 nm; this feature is likely to correspond to some aggregate species. As the AOT concentration increases from 1.6 to 8.3 μM, a gradual decrease of the new band at 490 nm is observed and the absorption spectrum adopts the expected form of a D_{2h} porphyrin with a well-defined Soret band at 419 nm and less intense Q bands at 517, 551, 597, and 654 nm. In addition, at [AOT] > 8.3 mM, it was also observed that the disappearance of the band at 490 nm associated with the appearance of a typical D_{2h} absorption spectrum is a time-dependent process (see Figure S5, Supporting Information). For this reason, all the experiments were performed after 3 h of stabilization. The emission spectrum is also highly sensitive to the addition of AOT. A gradual decrease of the emission band at 677 nm (with a shoulder near 740 nm) is accompanied by the appearance of two emission bands at 654 and 716 nm (Figure 6A). Well-defined *iso*-emissive points indicate two different excited state species in equilibrium that are controlled by the AOT concentration. The ratio of the fluorescence intensity of the fading and emerging bands (I_F(677 nm)/I_F(654 nm)) shows a linear correlation with AOT concentrations until [AOT] = 8.3 μM (Figure 6B). The fluorescence lifetimes also confirm the existence of different species in *iso*-octane/AOT mixtures. The fluorescence decays were best described by a sum of two exponential terms: a long-lived component of 9.6 ns and a short-lived component of 5.0 ns, similar to the ones obtained in organic solvents. The pre-exponential factors are also AOT concentration dependent. Figure 6B (inset) shows clearly the variation on the pre-exponential factors upon addition of AOT. The major differences are observed until AOT concentrations reach 10 μM.

3.4.2. Effect of the Water-to-Surfactant Ratio in AOT-iso-Octane-Water Reverse Micelles. Absorption and fluorescence emission from compounds **1** and **2** was measured in reverse micelles at different water-to-surfactant ratios. The surfactant concentration was kept constant, while the water concentration was allowed to change, varying the size of the reverse micelles. In AOT/water systems at ω_0 < 10, compound **1** shows similar absorption and emission bands. Main changes that are clearly represented in Figure 7A are observed in reverse micellar systems with water-to-surfactant ratios between 10 and 30. As ω_0 increases, the formation and increase of a new broad band at 470 nm is observed, at the expense of the maximum absorption of the main Soret band (419 nm, about 60% decrease), with a well-defined isosbestic point at 428 nm. The fluorescence spectra obtained at the same ω_0 values (Figure 7B) also show

dx.doi.org/10.1021/jp4076993 | J. Phys. Chem. B 2013, 117, 15023−15032

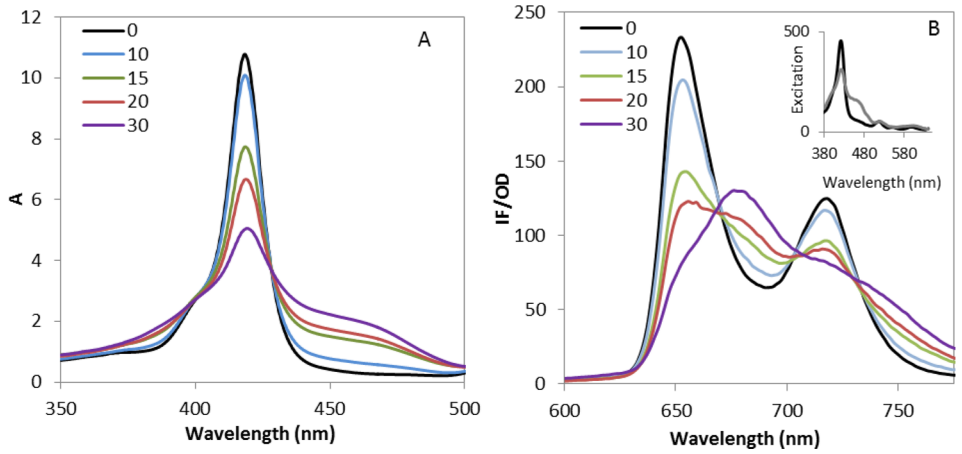

Figure 7. (A) Absorption and (B) fluorescence emission spectra of **1** (5 μM, λ_{exc} = 400 nm) in AOT reversed micelles at different ω_0 values. Inset: Excitation spectra obtained at (black) λ_{em} = 650 nm and (gray) λ_{em} = 725 nm.

similar changes in reverse micelles at higher water content. While below ω_0 < 10 only a small decrease in the emission bands is noticed, at ω_0 > 10, the disappearance of the initial fluorescence bands at 652 and 714 nm is followed by the appearance of a red-shifted band at 677 nm with a shoulder near 740 nm. The existence of two *iso*-emissive points at 665 and 702 nm (Figure 7B) shows that only two species in equilibrium are present in these solutions. Excitation data (inset in Figure 7B) obtained at 650 and 725 nm shows that the fluorescence emission at 650 nm comes almost exclusively from the Soret band, whereas the fluorescence excitation spectra at 725 nm almost match the absorption spectra, with a significant contribution of the new band at higher wavelengths. In particular, the emission spectra are not dependent on the excitation wavelength (400, 430, and 470 nm).

The fluorescence lifetimes were determined for **1** in reverse AOT/*iso*-octane micelles at increasing ω_0 values, and collected at λ_{em} = 650 nm and λ_{em} = 680 nm (see Figure S4, Supporting Information). A two exponential decay was always observed with a short lifetime of approximately 5 ns and a longer lifetime of approximately 10 ns. Nevertheless, the relative weights of the two components are fully dependent on the water content (Table 4).

4. DISCUSSION

Structures of β-Vinylpyridinium Porphyrins in Organic Solvents. It is well-known that the biological functions of porphyrins are dependent on the structures that they adopt due to interactions with different environments. The unique β-vinyl linker between the porphyrin and the pyridinium moieties confers to porphyrins **1** and **2** a higher degree of conjugation than a *meso* substitution and also the possibility of having the contribution of multiple structures, like the ones represented in Figure 8.

Those structures within selected microvicinities may influence the photophysical properties of β-vinylpyridinium porphyrins. In *trans* and *cis* structures, the positive charge is located on the pyridine nitrogen, while in the *quinoid* structure the positive charge is located in the pyrrolic nitrogen. It is then expected that diverse environments may interact differently with these two types of nitrogens.

The ground-state absorption behavior of compounds **1** and **2** in organic solvents is very complex with an additional red shift and broad band whose absorption intensities and wavelength maxima are quite dependent on the nature of the solvent and on the substitution pattern. The protonation of the inner core of the porphyrin and aggregation processes are two phenomena frequently described to induce such red shift bands in the ground state spectra. To ensure that acid−base equilibrium is irrelevant in our measurements, we have guaranteed that all the experiments were done in non-acidic solutions.[11] Also, the possibility of large aggregate formation was checked by means of RLS experiments,[12] and in all cases, the RLS spectra did not show enough intensity to overcome the absorption effects (data not shown). These results clearly demonstrate that the unusual spectroscopic behavior of compounds **1** and **2** in organic solvents is not due to the presence of aggregates.

It is worth mentioning that the new band red-shifted observed in the absorption spectra of porphyrins **1** and **2** is absent in the UV−vis spectra of their synthetic precursors (2-formyl-5,10,15,20-tetraphenylporphyrin,[13] 1,2-dimethylpyridinium iodide, and 1,4-dimethylpyridinium iodide), denoting that the features observed cannot be explained on the basis of a superimposition of the spectra of two isolated moieties. Thus, one can reasonably predict the existence of a clear electronic communication between the porphyrin ring and the pyridinium moiety through the vinylic bridge. In fact, these electronic absorption spectra resemble the ones reported for Ni(II), Zn(II), and Cu(II) complexes of β-conjugated porphyrins with strong acceptor groups.[14,15] Similar spectra were obtained by Screen et al.[16] when the electronic coupling of a zinc porphyrin

Table 4. Fluorescence Lifetimes and Pre-Exponential Factors of Compound 1 in AOT−*iso*-Octane Reverse Micelles

ω_o	τ_1 (ns)	A_1 (%)	τ_2 (ns)	A_2 (%)	χ^2
0[a]	4.9	13.5	10.3	86.5	1.33
10[a]	4.8	15.9	10.3	84.1	1.27
15[a]	4.6	20.5	10.2	79.5	1.24
20[a]	4.6	23.1	10.2	76.8	1.22
30[a]	4.2	30.6	9.7	69.4	1.26
0[b]	4.9	40.1	10.0	61.3	1.20
10[b]	4.7	46.0	10.0	54.0	1.21
15[b]	4.5	55.4	9.4	44.7	1.24
20[b]	4.5	57.3	9.4	42.7	1.18
30[b]	4.4	62.9	9.1	37.1	1.18

[a]$\lambda_{em.}$ = 650 nm. [b]λ_{em} = 680 nm.

dx.doi.org/10.1021/jp4076993 | J. Phys. Chem. B 2013, 117, 15023−15032

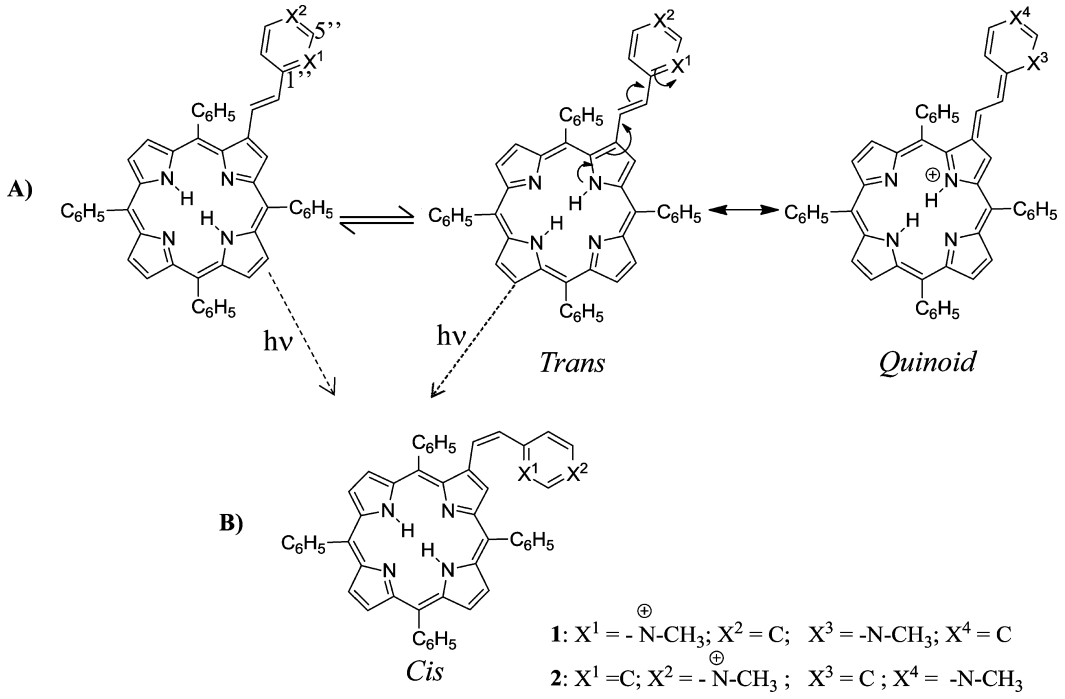

Figure 8. Possible structures adopted for (A) compounds **1** and **2** in the ground state and (B) compound **1** in the excited state.

and an aryl group linked to the *meso* position via azo, imine, alkene, and alkyne bridges was studied. On the basis of the widely split Soret band, large red shifts, and enhancement in the Q-band oscillator strength, they postulated that the azo link provides the strongest communication between the porphyrin and aryl moieties. To the best of our knowledge, no information has been provided concerning this effect on metal free porphyrins. Indeed, metal free *β*-styrylporphyrins structurally related to our porphyrins **1** and **2** are known to display typical porphyrin absorption spectra.[17] Therefore, in compounds **1** and **2**, the strength of the pyridinium acceptor should be the main reason for the differences encountered. On the other hand, TMPyP, with pyridinium substituents linked to the *meso* position, presents typical porphyrin absorption spectra. In this case, the linkage position of the acceptor groups directly connected to the porphyrin core dictates the degree of donor/acceptor interactions in the ground state.

The changes observed in the absorption and emission spectra of compounds **1** and **2** upon the variation of solvent polarity must therefore be associated to a charge transfer state. The extent of electron transfer is limited by the degree of rotation toward the styryl double bond that dictates the coplanarity of the system. The *ortho* methylpyridyl group in compound **1** is much more hindered to rotation than the *para* methylpyridyl group in compound **2**. Thus, a higher electronic coupling is predicted for compound **2**, as reflected by the higher intensity of the red shift absorption band. The steric hindrance effect is also clearly seen by a comparison of the emission profiles of **1** and **2**, since for compound **2** the solvatochromism is ruled by the solvent polarity (see Table 3) which is a typical signature of a charge transfer process.

Previous semiempirical calculations on the electronic charge distribution on carbon atoms of compound **1** account for a negative charge density on carbon C-1″ (Figure 8) adjacent to the vinylic double bond and to the positive pyridinium nitrogen.[18] In order to search for possible alterations in the ground state that could explain the puzzling spectral changes induced in alcoholic solvents, we acquired the ^{1}H NMR spectra of compounds **1** and **2** in deuterated chloroform and deuterated chloroform/methanol mixtures (Figures S6 and S7, Supporting Information), before and after irradiation. From those experiments, the high stability of the *trans* configuration for both isomers is clear. After methanol addition, some of the signals in the NMR spectra of compound **1** suffer significant shifts, particularly the signal due to the resonances of H-5″ (see Figure 8 for numbering and Figures S6 and S7, Supporting Information) of the pyridinium moiety. These results suggest that, in the ground state, the pyridinium moiety should be involved in a specific interaction within the protic solvent.

The emission data obtained for compound **1** in protic solvents reflects the existence of a specific interaction between compound **1** and alcohols, by contrast to compound **2**. The nature of this interaction is not fully understood, but similar effects were detected in the ground and excited states of TMPyP which affected the second vibronic of the fluorescence emission spectra.[19]

Upon excitation, photoisomerization may occur, leading to the formation of a *cis* structure. In compound **1**, the *cis* structure is probably stabilized by interaction with the *β*-pyrrolic electrons through an intermediate six-member ring structure, which is preferentially solvated by alcohols with an increasing number of methylene units. Thus, the electron transfer from the porphyrin to the pyridinium moiety will be inhibited due to the interruption of the resonance pathway. As a result, the emission spectrum of compound **1** has no longer the characteristics of the *quinoid* structure. This effect may be seen as the signature of the *ortho* isomer, since the *cis* configuration of the *para* isomer cannot be stabilized through *β*-pyrrolic interactions. On the other hand, the emission spectra of compound **2** do not display an increase in the intensity ratio of fluorescence vibronics, stressing that the photophysical properties of *β*-pyridinium porphyrins can be tuned by substitution of the position of the positive charge in the pyridinium moiety.

dx.doi.org/10.1021/jp4076993 | J. Phys. Chem. B 2013, 117, 15023−15032

On the basis of the above information, the analysis of the fluorescence lifetimes gave us a hint about the identification of the porphyrins' structures in organic solvents. Due to the increased contribution of the shorter lived component of 1.4 ns, observed for compound **1** in alcohols, and its absence in the fluorescence decays of compound **2**, the latter could be due to the contribution of the *cis* structure of **1** in the excited state. Similarly, taking into account the significant weight of the 4 ns component in the fluorescence decays of compound **2**, we may assume that it is associated to the contribution of the *quinoid* structure.

As regards compound **1**, further evidence of the above conclusion is sought from the analysis of the increasing AOT concentration effect on the pre-exponential factors of fluorescence lifetimes (Figure 6). The decrease of the short-lived lifetime component of 4 ns upon AOT concentration is accompanied by the disappearance of the unusual absorption red shift that is associated to the charge transfer structure. A possible explanation for this effect is the existence of an important electrostatic interaction between the anionic head of the surfactant and the positive charges of the pyridinium that turn the pyridinium moiety into a less deficient electron group. The resonance interaction between the two moieties is strongly affected by ion pair formation. Spectroscopically, these features result in the loss of the representative transitions of the charge transfer processes and in the appearance of typical D_{2h} absorption, fluorescence spectra, and fluorescence lifetimes (~10 ns) of monomeric porphyrins.

On a first glance of the porphyrin **1** and **2** structures, we were tempted to think that the less hindered positive charge of compound **2** could be more accessible to the formation of an ion pair with the negative heads of AOT. However, the absorption and emission spectra are essentially the same upon increasing AOT concentrations, indicating that the interaction with AOT is less favorable when the positive charge is located in the pyrrolic nitrogen. Therefore, given the high planarity of the *quinoid* structure, the photophysics of compound **2** is mainly ruled by the charge transfer process.

Biexponential fluorescence decays have been reported for TMPyP in water and in organic solvents. The origin of these two components has been the object of some controversy and discussion, prevailing two main theories: one that predicts the existence of a monomer−dimer equilibrium with fluorescence lifetimes varying from 1.3 to 3.7 ns for the monomer and 4.9−6.1 ns for the dimer.[20,21] Slightly different results were obtained by Kano et al.[22] and Kalyanasundaram et al.[23] that reported monoexponential decays in water with lifetimes of 4.1 and 6.0 ns, respectively, which were assigned to the TMPyP dimer. The other theory disproves the TMPyP self-assembly hypothesis and relates these two components with the high affinity of TMPyP for glass surfaces. Nonetheless, our results do not point to the existence of either aggregates or dimer formation in solution nor the affinity of β-vinylporphyrins **1** and **2** for glass surfaces was noticed.

AOT Reverse Micelles. The ground state behavior of compound **1** in AOT reverse micelles is significantly different from the one observed in aqueous and *iso*-octane solutions where this compound is sparingly soluble and only non-specific aggregates can be detected. In reverse micelles, the analysis of the absorption and emission spectra and fluorescence lifetime data shows that, above $\omega_0 = 10$, whereby reverse micelles are formed, occur the main spectral changes. The absorption and emission spectra of compound **1** in reverse micelles of low water content ($0 < \omega_0 < 10$) are quite similar to the ones obtained in AOT solutions. In this case, the porphyrin should be competing with water for AOT solvation and remains solubilized near the water−micelle interface. The increase in the polar environment[24] and the decrease in the micro-viscosity[25] sensed by these systems ($\omega_0 < 10$) should not affect the stability of the porphyrin−AOT ion pair formed. The invariance of the absorption and emission spectra in water-to-surfactant ratios up to 10 implies that compound **1** always experiences the same environment.

The differences observed in the absorption and emission spectra at ω_0 values larger than 10 clearly indicate a change in the porphyrin location related to the separation of bulk water. At these high water-to-surfactant ratios, all the polar head groups of AOT molecules are in contact or bound to water molecules. The hydrophobic characteristics of compound **1** should limit its affinity to bulk water. In fact, the ground state absorption spectrum resembles the one obtained in organic solvents. This result clearly indicates that porphyrin **1** should be preferentially located within the micellar external interface. Interestingly, the *para* isomer **2** does not incorporate in AOT reverse micelles and seems to remain essentially in the organic phase.

The disappearance of the unusual red shift band with AOT concentration and its reappearance after water addition are quite interesting results. Herein, we show that it is possible to control the charge flow through molecule demands, just manipulating the properties of the surrounding environment.

5. CONCLUSIONS

The electronic absorption and emission of two β-vinyl-pyridinium porphyrins, isomers differentiated as **1** (*ortho*) and **2** (*para*) as regards the position of the porphyrin linkage to the pyridinium moiety, were investigated in organic solvents and in AOT−*iso*-octane−water reverse micelles. An unusual red-shifted band appearing at 455−505 nm was detected in both isomers but was found considerably stronger in compound **2**. Fluorescence lifetime data and solvatochromic studies analyzed by the Kamlet−Taft multiparametric model emphasize the contribution of hydrogen bonding ability of compound **1** with polar solvents. The interactions of compounds **1** and **2** with the surfactant AOT are considerably different perhaps explaining the different virucidal effects observed.[3] We have used AOT reverse micelles as biomimetic models of the lipidic membrane for the encapsulated virus, and our results suggest that compounds **1** and **2** have different affinities toward membranes. While compound **1**, the cytotoxic compound, interacts with RMs, compound **2**, the non-cytotoxic one, does not. On the basis of these data, we believe that, *in vivo*, there is a strong interaction with the membrane virus reflected in the larger virucidal effect observed with the *ortho* isomer (compound **1**) as compared to the *para* isomer (compound **2**) which does not solubilize in the AOT. While no interaction is detected between the *para* isomer and AOT, the *ortho* isomer interacts with AOT solutions possibly through an ion-pair formation and in AOT reversed micelles should reside essentially at the interface/organic solvent away from the water pool.

Overall, the spectroscopic data lead us to propose the hypothesis that the two isomers have different contributions of the *trans* and *quinoid* resonance structures in the ground state. Compound **1** has a higher contribution of the *trans* structure which can isomerize in the excited state to the *cis* configuration,

dx.doi.org/10.1021/jp4076993 | J. Phys. Chem. B 2013, 117, 15023−15032

while in compound **2** the contribution of the *quinoid* structure is predominant.

■ ASSOCIATED CONTENT

Supporting Information

Raw absorption and emission spectra (Figure S1), deconvolution of the main absorption bands into Gaussian (Figure S2), correlation of electronic absorption maxima and solvent dielectric constants (Figure S3), data used to obtain the solvatochromic parameters without considering the spectrophotometer error (Table S1), representative fluorescence lifetime decays obtained for compounds **1** and **2** in organic solvents and in AOT reverse micelles (Figure S4), time-dependent process of compound **1** in AOT/*iso*-octane solutions: appearance of a typical D_{2h} absorption spectra (Figure S5), and NMR spectra of β-vinylpyridinium porphyrins (Figures S6 and S7). This material is available free of charge via the Internet at http://pubs.acs.org.

■ AUTHOR INFORMATION

Corresponding Author

*E-mail: sbcosta@ist.utl.pt.

Notes

The authors declare no competing financial interest.

■ ACKNOWLEDGMENTS

Thanks are due to Instituto Superior Técnico, Universidade Técnica de Lisboa (Pest-OE/QUI/UI0100/2011; Pest-OE/QUI/UI0100/2013), University of Aveiro, Portuguese Foundation for Science and Technology (FCT), European Union, QREN, FEDER, and COMPETE for funding the QOPNA research unit (project PEst-C/QUI/UI0062/2013). V.V.S. (SFRH/BPD/74270/2010) and E.M.P.S. (SFRH/BPD/66961/2009) are grateful to FCT for their post-doctoral grants.

■ REFERENCES

(1) *Handbook of Porphyrin Science*, Vols. *1*−*25*; Kadish, K. M., Smith, K. M., Guilard, R., Eds.; World Scientific Publishing Co: Singapore, 2010.

(2) Silva, E. M. P.; Giuntini, F.; Faustino, M. A. F.; Tomé, J. P. C.; Neves, M. G. P. M. S.; Tomé, A. C.; Silva, A. M. S.; Santana-Marques, M. G.; Ferrer-Correia, A. J.; Cavaleiro, J. A. S.; et al. Synthesis of Cationic b- Vinyl Substituted *meso*-Tetraphenylporphyrins and Their in Vitro Activity against *Herpes simplex* Virus Type I. *Bioorg. Med. Chem. Lett.* **2005**, *15*, 3333−3337.

(3) Silva, E. M.P.; Ramos, C. I. V.; Pereira, P. M. R.; Giuntini, F.; Faustino, M. A. F.; Tomé, J. P. C.; Tomé, A. C .; Silva, A. M. S.; Santana-Marques, M. G.; Neves, M. G. P. M. S.; Cavaleiro, J. A. S. Cationic β-Vinyl Substituted *meso*Tetraphenylporphyrins: Synthesis and NonCovalent Interactions with a Short Poly(dGdC) Duplex. *J. Porphyrins Phthalocyanines* **2012**, *16*, 101−113.

(4) Reichard, C. *Solvent and Solvent Effects in Organic Chemistry*, 2nd ed.; VCH: Weinheim, Germany, 1988.

(5) Dimroth, K.; Reichard, C.; Siepmann, T.; Bohlmann, F. *Liebigs Ann. Chem.* **1963**, *661*, 1.

(6) Hamlet, M. J.; Abboud, J. L; Taft, R. W. The Solvatochromic Comparison Method. The pi.* Scale of Solvent Polarities. *J. Am. Chem. Soc.* **1977**, *99*, 6027−6038.

(7) Reichard, C. Pyridinium-*N*-phenolate Betaine Dyes as Empirical Indicators of Solvent Polarity: Some New Findings. *Pure Appl. Chem.* **2008**, *80*, 1415−1432.

(8) Zulauf, M.; Eicke, H.-F. Inverted Micelles and Microemulsions in the Ternary System Water/aerosol-OT/isooctane as Studied by Photon Correlation Spectroscopy. *J. Phys. Chem.* **1979**, *83*, 480−486.

(9) Kinugasa, T.; Kondo, A.; Nishimura, S.; Miyauchi, Y.; Nishii, Y.; Watanabe, K .; Takeuchi, H. Estimation for Size of Reverse Micelles Formed by AOT and SDEHP Based on Viscosity Measurement. *Colloids Surf., A* **2002**, *204*, 193−199.

(10) Eicke, H. F.; Rehak, J. On the Formation of Water/Oil-Microemulsions. *Helv. Chim. Acta* **1976**, *59*, 2883−2891.

(11) Gouterman, M. *The porphyrins*; Dolphin, D., Ed.; Academic Press: New York, 1978.

(12) Collings, P. J.; Gibbs, E. J.; Starr, T. E.; Vafek, O.; Yee, C.; Pomerance, L. A.; Pasternack, R. F. Resonance Light Scattering and Its Application in Determining the Size, Shape, and Aggregation Number for Supramolecular Assemblies of Chromophores. *J. Phys. Chem. B* **1999**, *103*, 8474−8481.

(13) Bonfatini, E.; Burrell, A. K.; Campbell, W. M.; Crossley, M. J.; Gosper, J. J.; Harding, M. M.; Officer, D. L.; Reid, D. C.W. Efficient Synthesis of Free-Base 2-formyl-5,10,15,20-tetraarylporphyrins, Their Reduction and Conversion to [(Porphyrin-2-yl)methyl]phosphonium salts. *J. Porphyrins Phthalocyanines* **2002**, *6*, 708−719.

(14) Chin-Ti Chen, C.-T.; Yeh, H.-C.; Zhang, X. Yu. Olefin-Mediated Interaction Observed for Nickel Tetraphenylporphyrins with an Acceptor Substituted on the β-Carbon. *J. Org. Lett.* **1999**, *1*, 1767−1770.

(15) Walsh, P. J.; Gordon, K. C.; Wagner, P.; Officer, D. L. Resonance Raman Studies of β-Substituted Porphyrin Systems with Unusual Electronic Absorption Properties. *ChemPhysChem* **2006**, *7*, 2358−2365.

(16) Screen, T. E. O.; Blake, I. M.; Rees, L. H.; Clegg, W.; Borwick, S. J.; Anderson, H. L. Making Conjugated Connections to Porphyrins: a Comparison of Alkyne, Alkene, Imine and Azo Links. *J. Chem. Soc., Perkin Trans. 1* **2002**, 320−329.

(17) Bonfantini, E. E.; Burrell, A. K.; Officer, D. L.; Reid, D. C. W.; McDonald, M. R.; Cocks, P. A.; Gordon, K. C. Synthesis, Characterization, Structure, Electrochemistry, and Spectroscopy of Porphyrins That Have a Conjugated Connection to Donor/Acceptor Groups. *Inorg. Chem.* **1997**, *36*, 6270−6278.

(18) Izquierdo, R. A.; Barros, C. M.; Santana-Marques, M. G.; Ferrer-Correia, A.; Silva, E. M. P.; Giuntini, F.; Faustino, M. A. F.; Tomé, J. P. C.; Tomé, A. F.; Silva, A. M. S.; et al. Characterization of Isomeric Cationic Porphyrins with β-Pyrrolic Substituents by Electrospray Mass Spectrometry: The Singular Behavior of a Potential Virus Photoinactivator. *J. Am. Soc. Mass Spectrom.* **2007**, *18*, 218−225.

(19) Vergeldt, F. J.; Koehorst, R. B. M.; van Hoek, A.; Schaafsma, T. J. Intramolecular Interactions in the Ground and Excited States of Tetrakis(*N*-methylpyridyl)porphyrins. *J. Phys. Chem.* **1995**, *99*, 4397−4495.

(20) Kemnitz, K.; Sakagushi, T. Water-Soluble Porphyrin Monomer—Dimer Systems: Fluorescence Dynamics and Thermodynamic Properties. *Chem. Phys. Lett.* **1992**, *196*, 497−503.

(21) Brookfield, R. R.; Ellul, H.; Harriman, A. Luminescence of Porphyrins and Metalloporphyrins IX: Dimerization of *meso*-Tetrakis-(*N*-methyl-4-pyridyl)-porphine. *J. Photochem.* **1985**, *31*, 97−103.

(22) Kano, K.; Nakajima, T.; Takei, M.; Hashimoto, S. Self Aggregation of Cationic Porphyrin in Water. *Bull. Chem. Soc. Jpn.* **1987**, *60*, 1281−1287.

(23) Kalyanasundaram, K. Photochemistry of Water-Soluble porphyrins: Comparative Study of Isomeric Tetrapyridyl- and Tetrakis(*N*-methylpyridiniumyl)porphyrins. *Inorg. Chem.* **1984**, *23*, 2453−2459.

(24) Belletête, M.; Lachapellle, M.; Durocher, G. Polarity of AOT Micellar Interfaces: Use of the Preferential Solvation Concepts in the Evaluation of the Effective Dielectric Constants. *J. Phys. Chem.* **1990**, *94*, 5337−5341.

(25) Hasegawa, M.; Sugimara, T.; Shindo, Y.; Kitahara, A. Structure and Properties of AOT Reversed Micelles as Studied by the Fluorescence Probe Technique. *Colloid Surf., A* **1996**, *109*, 305−318.